A Harmonic Model of MMC Based on Nearest-Level Modulation With the Equidistant Controlled Firing Scheme

Xiaowen Chen[1], Zaibin Jiao[2],

[1] State Grid Henan Marketing Service Center (Metrology Center), Zhengzhou 450000, Henan Province, China
[2]School of Electrical Engineering，Xi'an Jiaotong University，Xi'an 710049，Shaanxi Province，China
E-mail: 2057652356@qq.com; jiaozaibin@mail.xjtu.edu.cn

Abstract With the rapid development of flexible DC transmission systems, the application of modular multilevel converter MMC is becoming increasingly widespread. Meanwhile, the nearest-level modulation is most applied. This paper establishes a simple and efficient harmonic model of MMC based on nearest-level modulation with the equidistant controlled firing scheme. First, based on the analysis of the working principle of MMC and the modulation principle, the Fourier decomposition of the stair wave is obtained. Then, according to the equivalent circuit diagram of MMC, the stair wave is exactly the differential-mode voltage. Moreover, the amplitude and phase of each differential-mode voltage harmonic content are obtained. So far, MMC can be regarded as a harmonic voltage source. Finally, simulations were performed on PSCAD to verify the accuracy of the MMC harmonic model proposed in this paper. Furthermore, the MMC harmonic model under the equidistant controlled firing scheme and real-time trigger control were also compared. The final results show that the model proposed in the paper can accurately reflect the harmonic characteristics of MMC in the existing power system after considering the equally-spaced trigger control.

***Index Terms*—modular multilevel converter， nearest-level modulation， equidistant controlled firing scheme， harmonic， Fourier principle**

I. INTRODUCTION

The modular multilevel converter (MMC) is a core equipment in flexible AC transmission systems. The MMC topology is highly modular and has the advantages of low losses, low output voltage harmonic distortion, and ease of scalability, making it a promising technology for a wide range of applications. However, the high voltage levels and complex modulation strategies of MMCs make harmonic analysis challenging at high control frequencies [2-7], which typically use nearest-level modulation (NLM) to approximate a sine modulation wave with a stair wave. MMCs with higher voltage levels and higher control frequencies generally have better harmonic characteristics. However, there is still a practical need for modeling MMC harmonics. In this paper, we analyze the harmonic characteristics of equidistant controlled firing scheme and the NLM modulation strategies. We propose an MMC harmonic model with time-domain discreteness, which is important for harmonic analysis and resonance suppression in hybrid AC/DC power systems.

Currently, most harmonic models for modular multilevel converters (MMC) are based on real-time trigger control [1], an idealized time-continuous triggering method that assumes the control frequency to be infinitely high. However, in practical power systems, the control frequency of the control system is a finite value, and this control method is called equidistant controlled firing scheme. Therefore, the time-domain discretization characteristic of equidistant controlled firing scheme challenges the harmonic modeling of MMC in actual power systems.

According to the topology of the modular multilevel converter (MMC), the electrical quantities, such as the capacitor voltage, submodule voltage, phase voltage, and inter-phase circulating current, are solved using the IGBT switch function model in reference [5]. The voltage analytical expressions only contain low-frequency 2^{nd}, 3^{rd}, and 4^{th} harmonic components while ignoring the high-order harmonic components. Reference [6] establishes a frequency-domain impedance model for small disturbances based on the continuous MMC model's positive and negative sequence decomposition. The DC-side impedance is viewed as a series connection of RLC passive elements, and the AC-side impedance is composed of fixed and variable impedances. However, the mathematical, analytical

expression of the harmonic impedance model is too complex to compute and cannot be simulated by components. Moreover, the impedance frequency characteristics under voltage and current excitation are different and have no obvious regularity, making it difficult to apply in practice. Reference [7] derives the MMC harmonic model's frequency-domain expression based on the Lu-Xi power project's simplified control transfer function and equivalent to the converter as a harmonic current source parallel impedance in engineering applications. Although this model highly depends on complex actual control parameters and can accurately reflect the harmonic characteristics of MMC, its modeling complexity limits its promotional value. References [8-12] are all based on the principle of staircase wave modulation. They derive the mathematical expressions of staircase waves under real-time trigger control by averaging the switch function and Fourier series decomposition. However, due to the idealized characteristics of real-time trigger control, it can only be used for simplified qualitative analysis and cannot consider the engineering reality too much.

In summary, previous literature on the harmonic characteristics analysis of MMC has certain limitations [1-16]. The time-domain analytical method based on the switch function obtains the Fourier series of the ideal stair wave. This idealized time-domain continuous model does not match the engineering system. The time-domain simulation method is very slow due to the highly modularized structure of the MMC. The frequency-domain analytical method that considers the complex and detailed control system is difficult to implement due to the difficulty obtaining control parameters. Therefore, it is urgent to establish a simple, efficient, and practically applicable harmonic model for MMC under equidistant controlled firing scheme in actual power systems.

The first part of this paper provides a detailed analysis of the topology, working principle, and nearest-level approximation modulation principle of the Modular Multilevel Converter (MMC). In the second part, starting from the stair wave, the Fourier expansion of the stair wave is derived through Fourier decomposition. Meanwhile, based on the simplified equivalent circuit diagram of the MMC, the expression for the differential-mode voltage is obtained, and the harmonic equivalent circuit diagram of the power system containing the MMC is analyzed. Finally, in the third part, the proposed harmonic model of the MMC under equidistant controlled firing scheme is validated through PSCAD simulation experiments. Moreover, a comparative analysis is conducted between the proposed harmonic model and the real-time trigger control harmonic model of the MMC proposed in previous studies.

II. Principle of Operation of Modular Multilevel Converter (MMC)

A. Main Circuit Topology

The modular multilevel converter (MMC) circuit is highly modular, as shown in Figure 1. Each phase of the three-phase MMC consists of two bridge arms, namely upper and lower arms, resulting in six bridge arms. Each bridge arm comprises an inductor and N submodules (SM) connected in series. The bridge arm inductor suppresses the circulating current between phases and the impact current during faults. The most common submodule uses a half-bridge topology. Each submodule can be equivalently modeled as a fully controllable switch, which outputs a DC-side capacitor voltage of U_C or 0. By controlling the switch of each submodule, a stair wave is generated to approximate a sine wave.

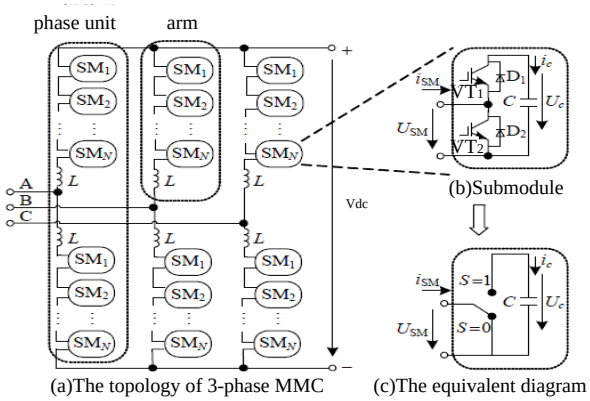

Fig.1 The topology of MMC

The submodule comprises two fully controllable power electronic devices, VT1 and VT2, two anti-parallel diodes D1 and D2, and a DC-side energy storage capacitor C, forming a half-bridge unit. The submodule has a and b connection ports for series connection to the main circuit, and it has three operating states as shown in Figure 2: the locked state where both VT1 and VT2 are turned off, the turn-on state where VT1 is conducting and VT2 are turned off, and the turn-off state where VT1 is turned off and VT2 is conducting.

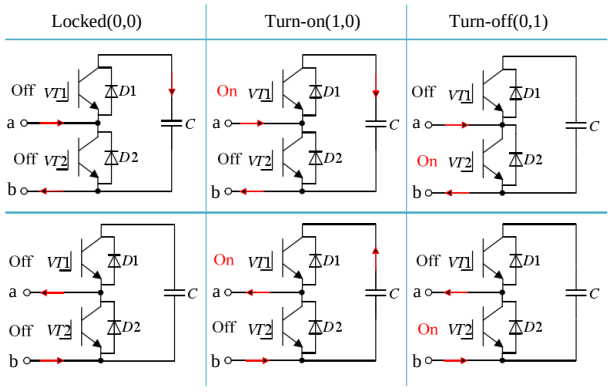

Fig.2 The 3 operating states of submodule

Each operating state has two operating modes, as shown in Table 1: current flows from a to b; current flows from b to a.

Tab.1 The 6 statues of submodule

Working state	VT_1	VT_2	D_1	D_2	Current Flow	U_{sm}	Capacitive state
Locked	**0**	**0**	**1**	**0**	**a to b**	**Uc**	**Charging**

			0	1	b to a	0	Bypass
Turned on	1	0	1	0	a to b	Uc	Charging
			0	0	b to a	Uc	Discharging
Turned off	0	1	0	0	a to b	0	Bypass
			0	1	b to a	0	Bypass

(Note: 1 represents the turn-on state, 0 represents the turn-off state)

The MMC supports the voltage of the DC bus (V_{dc}) by the DC-side capacitor voltage of each submodule (U_C). At any time, a total of N submodules are engaged in each phase of the MMC. That is, the MMC satisfies the following characteristics:

$$n_{pj} + n_{nj} = N \tag{1}$$

$$V_{dc} = NU_C \tag{2}$$

where j represents phase A, B, or C; n_{pj} and n_{nj} are the number of submodules that need to be engaged in the upper and lower bridge arms of phase j, respectively; N is the number of submodules in each arm (upper and lower arms have the same number of submodules), which is usually an even number; V_{dc} is the DC voltage value; U_C represents the submodule DC-side capacitor voltage.

The number of active submodules in a single bridge arm can be 0, 1, 2…N. Usually, N is an even number so that the number of active submodules in the upper and lower bridge arms is equal. When it equals to N/2, the phase voltage is zero. Therefore, an MMC with N submodules in each arm can output up to (N+1) voltage levels, $0、\pm U_C、\pm 2U_C、\cdots、\pm\frac{N}{2}U_C$, when the DC-side midpoint is the zero voltage level.

B. Principle of Nearest-Level Modulation

Recently, nearest-level modulation (NLM) has become the most commonly used stair wave modulation strategy, as shown in Figure 3. As the instantaneous value of the modulation wave rises from zero, the number of submodules in the lower bridge arm of the corresponding phase unit that is in the on-state needs to gradually increase, while the number of submodules in the upper bridge arm in the on-state needs to correspondingly decrease, so that the output voltage of the phase unit follows the rise of the modulation wave. As the instantaneous value of the modulation wave starts to decrease from its maximum value, the situation is reversed. Since the direct voltage of the submodule (U_C) is the smallest voltage unit, the value of the stair wave can only be a multiple of U_C, and it is the nearest integer approximation value of the sine modulation wave. NLM tracks the sine modulation wave by switching the direct voltage level of the submodules on and off to generate the output wave.

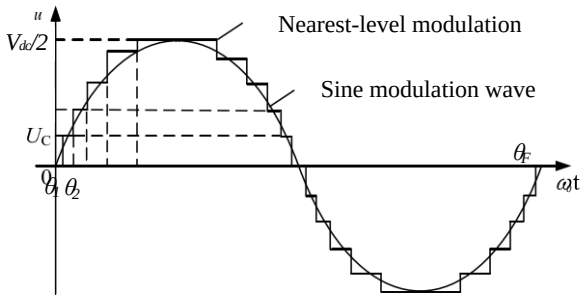

Fig.3 The diagram of nearest-level modulation (NLM)

In practical operation, the control system of MMC updates the trigger signals every control period T_{ctrl}. For an MMC with N submodules in a bridge arm, when the control system starts from any moment t_0 (θ_1 relative to the phase angle of the sine modulation wave). In every control period, the number of submodules for each arm is updated according to equations (1) and (2):

$$n_{pj}(t+T_{ctrl}) = \frac{N}{2} - round(\frac{u_{vj}(t+T_{ctrl})}{U_C}) \tag{3}$$

$$n_{nj}(t+T_{ctrl}) = \frac{N}{2} + round(\frac{u_{vj}(t+T_{ctrl})}{U_C}) \tag{4}$$

$(0 \le n_{pj}、\ n_{nj} \le N)$

where u_{vj} is the instantaneous value of the j phase modulation wave, T_{ctrl} represents the control period, and $round(x)$ represents the nearest integer to x, which satisfies the rounding rule.

After determining the number of active submodules in the upper and lower arms, triggering signals are sent to the corresponding submodules in conjunction with the capacitance voltage balancing strategy, so that the output voltage of the MMC is the closest to the instantaneous sine modulation wave.

Based on the modulation wave and the NLM algorithm, the output stair waves of the MMC with different numbers of submodules can be obtained. The stair wave does not necessarily experience a transition every control cycle T_{ctrl}, nor does it necessarily change U_C by one step during a transition. When the control cycle T_{ctrl} is finite, NLM can ensure that the difference between the stair wave and the sine modulation wave is controlled within $\pm\frac{U_C}{2}$ at control cycle points, but it cannot guarantee the difference to be controlled within $\pm\frac{U_C}{2}$ at all time points, hence there is a time delay in the approximation of the stair wave to the modulation wave under a limited control frequency. Discreteness and lag are inherent characteristics of equidistant controlled firing scheme. As the control frequency increases and the control

cycle T_{ctrl} decreases, the delay decreases.

When the control frequency is infinite, the control period T_{ctrl} is 0. As long as the difference between the modulation wave and the stair wave reaches $\pm\frac{U_C}{2}$, the stair wave will jump once, and the jump value is U_C. The difference between the stair wave and the sine modulation wave is controlled within $\pm\frac{U_C}{2}$ at any time. This trigger mode of the NLM modulation is called real-time trigger control, which has continuity and ideal features. At this case, the output voltage of the MMC is an ideal stair wave that best approximates the sine modulation wave.

III. HARMONIC MODEL OF MMC

A. Fundamental Assumptions

This model is established under the steady-state operating condition, and all theoretical derivations are based on the following assumptions:

1. The modulation waves of the three phases are standard sine waves, with a phase shift of 120 degrees in sequence.
2. The MMC adopts an appropriate capacitance equalization strategy to ensure slight DC-side capacitor voltage fluctuation of the submodules.
3. The MMC adopts equidistant controlled firing scheme.

B. Derivation of Harmonic Analytical Expressions

Firstly, a stair wave is composed of F rectangular waves, F represents the carrier ratio, which is equal to the ratio of the control frequency to the fundamental frequency and also equal to the ratio of the fundamental period to the control period, $F=\frac{f_{ctrl}}{f_0}=\frac{T_0}{T_{ctrl}}$. The harmonic analysis method will decompose the stair wave into Fourier components, transforming it into the Fourier components of the F rectangular waves that make up the stair wave.

The stair wave and its rectangular waves are both periodic waves with a period of one fundamental period of 20ms. Within one fundamental period, the triggering signal is updated every control period. Therefore, one period contains F control time points, whose phases are respectively θ_1、$\theta_2\cdots\theta_F$ relative to the sine modulation wave. Under equidistant controlled firing scheme, the stair wave does not satisfy the odd symmetry condition.

Taking the A-phase stair wave of the five-level MMC as an example. When the carrier ratio is 9, the control system updates the trigger signal nine times in one fundamental period, and the control time points are θ_1、$\theta_2\cdots\theta_9$, respectively. The A-phase stair wave voltage is u_a, the number of active submodules in the upper arm is n_{pa}, and the number of active submodules in the lower arm is n_{na} during different periods within one fundamental period shown in Table 2. Meanwhile, the submodule ON/OFF states of the five-level MMC satisfy equations (1) and (2).

Tab.2 The different statues of submodule in A-phase of 5-level MMC(F=9)

Time	θ_1–θ_2	θ_2–θ_3	θ_3–θ_4	θ_4–θ_5	θ_5–θ_6	θ_6–θ_7	θ_7–θ_8	θ_8–θ_9	θ_9–$2\pi+\theta_1$
u_a	U_C	$2U_C$	$2U_C$	U_C	0	$-U_C$	$-2U_C$	$-2U_C$	$-U_C$
n_{pa}	1	0	0	1	2	3	4	4	3
n_{na}	3	4	4	3	2	1	0	0	1
N	4	4	4	4	4	4	4	4	4
V_{dc}	$4U_{dc}$	$4U_{dc}$	$4U_{dc}$	$4U_{dc}$	$4U_{dc}$	$4U_{dc}$	$4U_{dc}$	$4U_{dc}$	$4U_{dc}$

The A phase stair wave of five-level MMC under NLM modulation is considered as a combination of a series of rectangular waves, as shown in Figure 4.

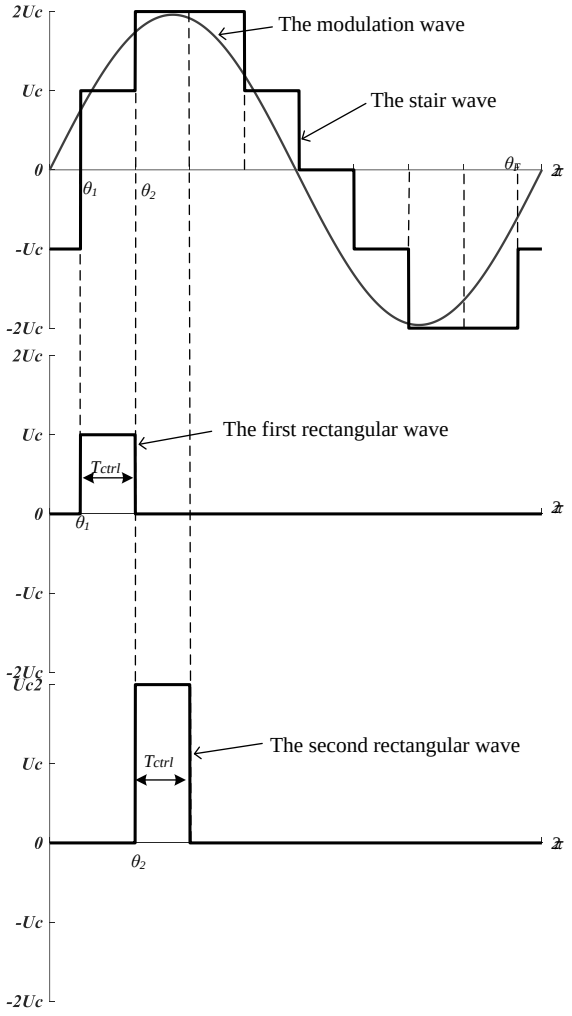

Fig.4 The stairs-wave of 5-level MMC (F=9)

Assuming the analytical expression of phase A modulation wave is:

$$u_{va}(t)=U_v\sin(\omega_0 t) \tag{5}$$

where U_v represents the amplitude of the modulation wave, and ω_0 represents the fundamental angular frequency.

The expression of the k th rectangular wave in Figure 4 is:

$$f_k(t)=\begin{cases}0 & 0<\omega_0 t<\theta_k\\ A_k & \theta_k<\omega_0 t<\theta_{k+1}\\ 0 & \theta_{k+1}<\omega_0 t<2\pi\end{cases} \tag{6}$$

where the three elements of the rectangular wave are included: the start time θ_k, the end time θ_{k+1} (actually referring to the width T_{ctrl}), and the height A_k ($k=1、2、\cdots、F$).

According to the equidistant controlled firing scheme and the nearest-level modulation, the following relationship is satisfied:

$$\theta_k=\theta_1+\frac{2\pi}{T_0}(k-1)T_{ctrl}=\theta_1+\frac{2\pi}{F}(k-1) \tag{7}$$

$$A_k=round(\frac{U_v\sin\theta_k}{U_c})U_c \tag{8}$$

Define the modulation ratio of the MMC as m, which equals the amplitude of the modulation wave divided by the half of DC voltage value. The expression for the modulation ratio is:

$$m=\frac{U_v}{V_{dc}/2} \tag{9}$$

After substituting equations (2) and (9) into equation (8), the expression for the amplitude of the rectangular wave is obtained:

$$A_k=round(\frac{1}{2}mN\sin\theta_k)\frac{V_{dc}}{N} \tag{10}$$

The Fourier series expansion expression of the k th rectangular wave is: （$k=1、2、\cdots、F$）

$$\begin{aligned}f_k(t)=A_k\{\frac{1}{F}+\sum_{n=1}^{\infty}\frac{1}{n\pi}[(\sin n\theta_{k+1}-\sin n\theta_k)\cos n\omega_0 t\\ -(\cos n\theta_{k+1}-\cos n\theta_k)\sin n\omega_0 t]\}\end{aligned} \tag{11}$$

The rectangular waves are superimposed. Then the Fourier series expansion expression of the phase A stair wave is obtained, as shown in Equation (12).

From Equation (12), the amplitude and phase expressions of the n[th] harmonic in the MMC stair wave voltage can be obtained as shown in Equations (13-14):

$$\begin{aligned}u_{staira}(t)&=f_1(t)+f_2(t)+\cdots+f_k(t)+\cdots+f_F(t)\\ &=\sum_{k=1}^{F}\left\{round[\frac{1}{2}mN\sin\theta_k]\frac{V_{dc}}{N}\{\frac{1}{F}+\sum_{n=1}^{\infty}\frac{1}{n\pi}[(\sin n\theta_{k+1}-\sin n\theta_k)\cos n\omega_0 t-(\cos n\theta_{k+1}-\cos n\theta_k)\sin n\omega_0 t]\}\right\}\end{aligned} \tag{12}$$

$$U_{\text{stair\_}n}=\frac{V_{dc}}{nN\pi}\sqrt{[\sum_{k=1}^{F}round(\frac{1}{2}\text{mNsin}\,\theta_k)(\text{sinn}\,\theta_{k+1}-\text{sinn}\,\theta_k)]^2+[\sum_{k=1}^{F}round(\frac{1}{2}\text{mNsin}\,\theta_k)(-\text{cosn}\,\theta_{k+1}+\text{cosn}\,\theta_k)]^2} \tag{13}$$

$$PH_{\text{stair\_}n}=arc\tan\frac{\sum_{k=1}^{F}round(\frac{1}{2}\text{mNsin}\,\theta_k)(\text{sinn}\,\theta_{k+1}-\text{sinn}\,\theta_k)}{\sum_{k=1}^{F}round(\frac{1}{2}\text{mNsin}\,\theta_k)(-\text{cosn}\,\theta_{k+1}+\text{cosn}\,\theta_k)} \tag{14}$$

where n represents the n[th] harmonic.

$$\begin{cases}\theta_k=\theta_1+(k-1)\dfrac{2\pi}{F}\\ \theta_{k+1}=\theta_1+\dfrac{2\pi}{F}k\end{cases} \tag{15}$$

Similarly, the B and C phase modulation waves lag behind the A phase by 120° and 240°, respectively. The Fourier series expansion of their stair waves are both similar to that of the A phase.

For MMC based on the nearest-level modulation with equidistant controlled firing scheme, this harmonic analysis method only utilizes five data: modulation ratio m, carrier ratio F, DC-side voltage V_{dc}, number of bridge arm submodules N, and initial triggering time corresponding to electrical angle θ_1. By substituting them into Equation (12), the harmonic contents of the output stair wave can be obtained.

C. Harmonic Equivalent Circuit of MMC

The MMC single-phase equivalent circuit is shown in Figure 5. The bridge arm impedance in the MMC is directly connected in series with the bridge arm, unlike in traditional two-level converters where it is connected between the converter and the AC system [1].

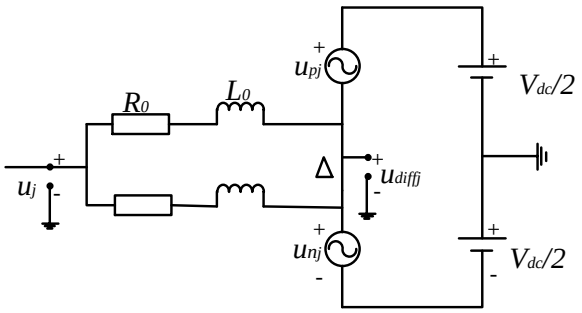

Fig.5 The single-phase equivalent model of MMC

The stair wave represented by equation (12) actually refers to the voltage at the virtual equipotential point Δ between the upper and lower bridge arms of phase A, that is, the differential-mode voltage u_{diffa} , which satisfies the following equation:

$$u_{stairj} = u_{diffj} = \frac{1}{2}(u_{nj} - u_{pj}) \tag{16}$$

where, j represent phases A, B, and C, respectively; u_{stairj} is the stair wave voltage of phase j; u_{diffj} is the differential-mode voltage of phase j; u_{pj} and u_{nj} are the voltages of the upper and lower bridge arms of phase j, respectively.

Therefore, looking into the AC-side port, the MMC can be equivalent to a harmonic voltage source $u_{diff\_n}(t)$ series with the bridge arm impedance of the equivalent harmonic model. Then, the AC-side port is connected to the n[th] harmonic network via the converter transformer T (and $u_{diff\_n}(t) = u_{stair\_n}(t)$). Thus, the equivalent model of the n[th] harmonic system including MMC is shown in Figure 6.

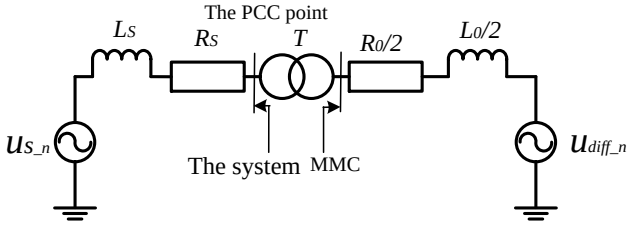

Fig.6 The equivalent harmonic model of n[th] network including MMC

IV. Simulation

A two-terminal MMC-HVDC system was constructed on PSCAD as shown in Fig. 7. The system has a capacity of 60 MVA, and both AC side voltages are 20 kV, while the DC side voltage is 20 kV. The upper and lower arms of the MMC each have 20 submodules, and the MMC adopts NLM modulation strategy under the equidistant controlled firing scheme.

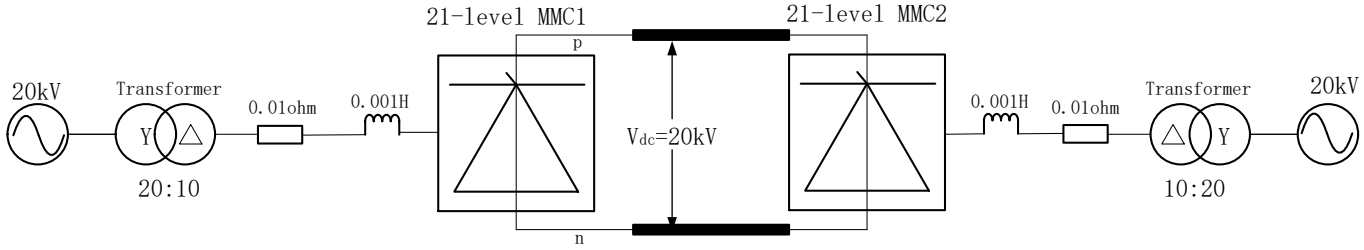

Fig.7 The system of 2-terminal MMC-HVDC

When the model is in steady-state operation, the two MMC stations' control frequency was changed simultaneously, resulting in five operating states with specific parameters shown in Table 3.

Tab.3 The parameters of MMC1 in state operations with different control frequencies

	Number of upper/lower bridge arm submodules(N)	Control frequency (f_{ctrl}/Hz)	Carrier ratio(F)	Modulation ratio(m)	DC voltage (V_{dc}/kV)	Initial trigger Angle (θ_1)
Case1	20	1000	20	0.8028	19.9611	0
Case2		1050	21	0.8026	19.9508	
Case3		1100	22	0.8074	19.8368	
Case4		1150	23	0.8057	19.8910	
Case5		1200	24	0.8093	19.7994	

The electromagnetic simulation results of the 5 cases were analyzed by Discrete Fourier Transform (FFT) to obtain the harmonic content of the differential-mode voltage of MMC1. Then, the parameters of the 5 cases were substituted into Equation (13) to calculate the harmonic content of the harmonic model. The comparison between the simulation result and the model calculation results is shown in Figure 8.

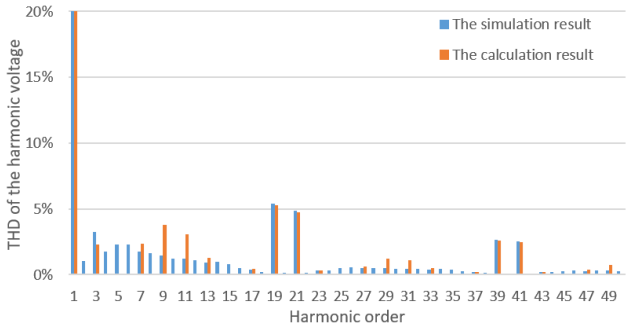

(a) The comparison diagram of MMC harmonic model when the control frequency is 1000Hz

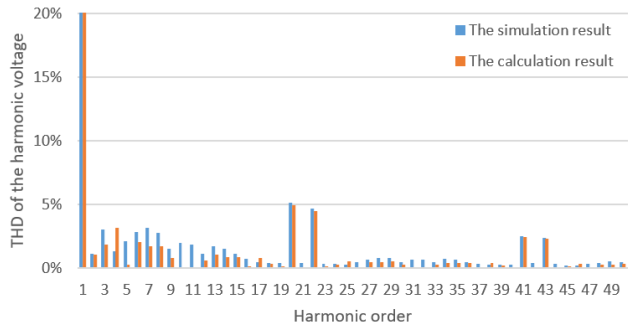

(b) The comparison diagram of MMC harmonic model when the control frequency is 1050Hz

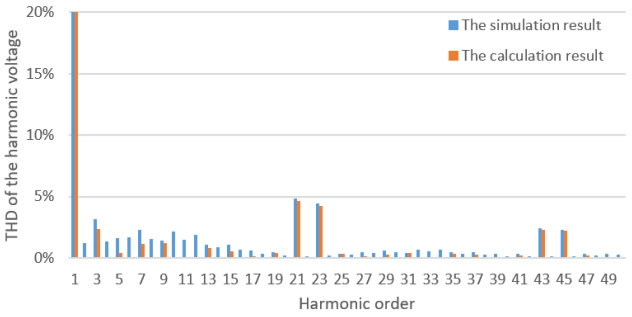

(c) The comparison diagram of MMC harmonic model when the control frequency is 1100Hz

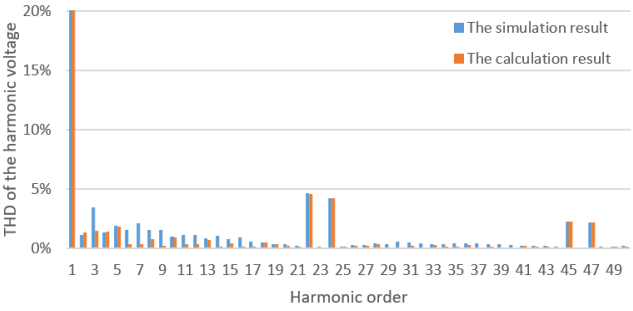

(d) The comparison diagram of MMC harmonic model when the control frequency is 1150Hz

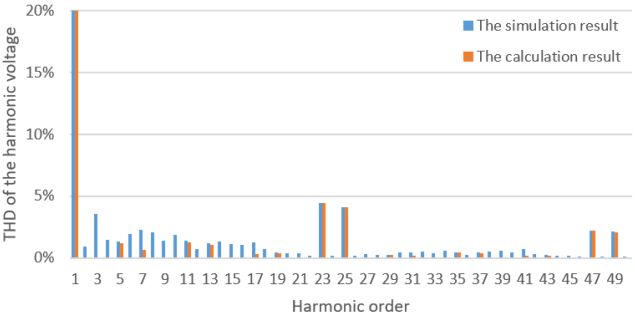

(e) The comparison diagram of MMC harmonic model when the control frequency is 1200Hz

Fig.8 The comparison of the harmonics between PSCAD and the model formula

Meanwhile, the total harmonic distortion (THD) of the harmonic voltage is used to measure whether the MMC harmonic model under the equidistant controlled firing scheme is closer to the simulation model compared with the MMC harmonic model under real-time trigger control. The comparison results of the THD of the three models are shown in Table 4. The MMC model under real-time trigger control uses the formula in reference [9].

Tab.4 The comparison of MMC's harmonic models between equidistant controlled firing scheme and real-time trigger control by THD

THD	Case1	Case2	Case3	Case4	Case5
Simulation	10.91%	11.56%	10.39%	9.83%	10.06%
Harmonic model under the equidistant controlled firing scheme	10.70%	9.83%	8.35%	8.16%	7.38%
Harmonic model under real-time trigger control	4.30%	4.30%	4.20%	4.24%	4.17%

In conclusion, the following results can be drawn:

(a) The MMC harmonic model under the equidistant controlled firing scheme proposed in this paper has significant features: the harmonic distribution is influenced by the control frequency, and the harmonics mainly distribute near the control frequency and its multiples, especially when the frequency is $kf_{ctrl} \pm f_0$, the harmonic content is relatively large (f_{ctrl}、f_0 represents the control frequency and the fundamental frequency, respectively; k is a positive integer);

(b) The frequency spectrum of the NLM-modulated MMC harmonic model under the equidistant controlled firing scheme has a small error compared with the electromagnetic simulation model, and the harmonic model under the equidistant controlled firing scheme reflects the distribution law and variation trend of the MMC harmonics well;

(c) From the perspective of the total harmonic distortion rate THD, the MMC harmonic model under the equidistant controlled firing scheme is closer to the electromagnetic simulation model, while the MMC model under the real-time trigger control has a large difference from the electromagnetic simulation model.

Therefore, the MMC harmonic model proposed in this paper can more accurately reflect the actual harmonic characteristics of the MMC in the power system after considering the equidistant controlled firing scheme.

V. CONCLUSION

Based on a detailed analysis of the topology, working principle, and modulation strategies of the nearest-level modulation (NLM), this paper focuses on the characteristic of the NLM modulation strategy under the equidistant controlled firing scheme, decomposes the generated stair wave into a series of related rectangular waves, simplifies the Fourier decomposition process of the stair wave, and

ultimately obtains the amplitude and phase expressions of each harmonic component of the MMC differential-mode voltage. Thus, MMC can be regarded as a harmonic voltage source. Furthermore, this paper analyzes the equivalent harmonic circuit model of a power system containing MMC, which will help to analyze the harmonic and resonance suppression calculations of AC/DC hybrid power systems.

To validate the accuracy of the proposed harmonic model, PSCAD simulation experiments were conducted to compare the electromagnetic simulation results of a 21-level MMC-HVDC system with the harmonic model under the equidistant controlled firing scheme and the harmonic model under real-time trigger control. The final results show that the proposed MMC harmonic model can more accurately reflect the harmonic characteristics of the actual power system MMC after considering the equidistant controlled firing scheme.

REFERENCES

[1] XU Zheng，et al．Flexible HVDC System [M]．Beijing：China Machine Press，2016：24-38．

[2] LV Jing，CAI Xu，ZHANG Jianwen．AC- and DC-side impedance models of modular multilevel converter[J]．Electric Power Automation Equipment，2017，37(1)：131-136．

[3] Jingwei Zhu．Research on the Control Strategy of Modular Multilevel Converter[D]．Xuzhou：China University of Mining and Technology，2017．

[4] Qiang Song，Wenhua Liu，Xiaoqian Li，et al．A Steady-State Analysis Method for a Modular Multilevel Converter[J]．IEEE TRANSACTIONS ON POWER ELECTRONICS，2013，28(8)：3702-3712．

[5] XUE Yinglin，XU Zheng，ZANG Zheren，et al．Analysis on Converter Impedance-frequency Characteristic of the MMC-HVDC System[J]．Proceedings of the CSEE，2014，34(24)：4040-4048．

[6] Changyue Zou，Hong Rao，Shukai Xu，et al．Analysis of Resonance Between a VSC-HVDC Converter and the AC Grid[J]．IEEE TRANSACTIONS ON POWER ELECTRONICS，2018，33(12)：10157-10167．

[7] GUAN Min-yuan，XU Zheng，PAN Wei-yong，et al．Analysis Calculation of Fundamental Wave and Harmonic Characteristics of Nearest Level Modulation[J]．High Voltage Engineering，2010，36(5)：1327-1332．

[8] GUAN Minyuan，XU Zheng，TU Qingrui，et al．Nearest Level Modulation for Multilevel Converters in HVDC Transmission[J]．Autmation of Electric Power Systems，2010，34(2)：48-52．

[9] Nguyen Phuc Huy．Research on Harmonic Characteristics of VSC-HVDC[D]．Beijing：North China Electric Power University，2015．

[10] XU Bin，ZHOU Shijia，LIN Weixing，et al．Analysis of Harmonic on the AC Side of MMC Based on Harmonic Equivalent Circuit and Fast Simulation Model[J]．Smart Grid，2016，4(3)：1327-1332．

[11] LI Peng-peng，GUO Jia-hu，LIANG Ke-jing．Analysis of harmonic characteristics for nearest level modulation based on MMC[J]．High Voltage Engineering，2014，38(4)：759-763．

[12] Xiao H Q，Xu Z，Xue Y L，et al．Theoretical analysis of the harmonic characteristics of modular multilevel converters [J]．Sci China Tech Sci，2013，56：2762–2770．

[13] XU De-zhi，WANG Fei，RUAN Yi，et al．Output impedance modeling and harmonic interactions of multiple inverters grid-connected system[J]．Electric Machines and Control，2014，18(2)：1-7．

[14] ZHANG Zheren，XU Zheng，XUE Yinglin．Calculation of DC Side Harmonic Currents for LCC-MMC Hybrid HVDC Transmission System[J]．Automation of Electric Power Systems，2014，38(23)：65-70．

[15] Haiwei Zhao. Research on STATCOM Based on MMC in Low and Medium Voltage of the Distribution Network[D]．Nanjing：Nanjing University of Aeronautics and Astronautics，2016．

[16] Manuel Madrigal Martinez．Modelling of Power Electronics Controllers for Harmonic Analysis in Power Systems[D]．Glasgow，Scotland，U.K.：The University of Glasgow，2001．

[17] RAO Hong，SONG Qiang，LIU Wenhua．Optimized Design Solution for Multi-terminal VSC-HVDC System Using Modular Multilevel Converters and Comparison [J]．Automation of Electric Power Systems，2013，37(15)：103-108．

[18] LUO Yu，RAO Hong，XU Shukai，et al．Efficient Modeling for Cascading Multilevel Converters[J]．Proceedings of the CSEE，2014，34(15)：2346-2352．

[19] LUO Yu，SONG Qiang，RAO Hong．An Optimized Design Method of Cascade Number for Sub-modules in Modular Multilevel Converters [J]．Automation of Electric Power Systems，2013，37(4)：114-118．

[20] Su Jianshen，Guo Jingdong，Jin Tao．DC Fault Characteristics and Line Fault Recovery Strategy in Flexible DC Power Network[J]．TRANSACTIONS OF CHINA ELECTROTECHNICAL SOCIETY，2019．

[21] Yuejuan Bia．Study on Normal Modular Multilevel Converter

and Its Control Strategy[D] . Guangzhou : South China University of Technology, 2016 .